CONCURRENCY AND COMPUTATION: PRACTICE AND EXPERIENCE
Concurrency Computat.: Pract. Exper. 0000; 00:1–20
Published online in Wiley InterScience (www.interscience.wiley.com). DOI: 10.1002/cpe

Reconstructing 3D Virtual Environments within a Collaborative e-Infrastructure

Gianpaolo Coro[1*], Marco Palma[2], Anton Ellenbroek[3], Giancarlo Panichi[1], Thiviya Nair[2], Pasquale Pagano[1]

[1]Istituto di Scienza e Tecnologie dell'Informazione "Alessandro Faedo" – CNR, Pisa, Italy
[2]Dipartimento di Scienze della Vita e dell'Ambiente (DISVA), Universitá Politecnica delle Marche, Ancona, Italy
[3]Food and Agriculture Organization of the United Nations (FAO), Rome, Italy

SUMMARY

Sets of two dimensional images are insufficient to capture the development in time and space of three-dimensional structures. The 2D 'flattening' of photographs results in a significant loss of features especially if the photos were taken by one person. Automatically collecting and aligning photos in order to render 3D structures from 2D images without specialized equipment, is currently a complex process that requires specialist knowledge with often limited results. In this paper, an Open Science oriented workflow is proposed where an on-line file system is used to share photos of an object or an environment and to produce a virtual reality scene as a navigable 3D reconstruction that can be shared with other people. Our workflow is based on a distributed e-Infrastructure and overcomes common limitations of other approaches by having all the used technology integrated on the same platform and by not requiring specialist knowledge. A performance evaluation of the 3D reconstruction process embedded in the workflow is reported against a commercial software and an open-source software in terms of computational efficiency and reconstruction accuracy, and three marine science use cases are reported to show potential applications of the workflow.

Received …

KEY WORDS: Photogrammetry, 3D Reconstructions, Virtual Reality, e-Infrastructures, Cloud Computing, Photography, Virtual Research Environments, Open Science

1. INTRODUCTION

Measuring the dynamics of change in environments over time through photos can be important to monitor the effects of external stressors on ecological systems. For example, ocean acidification impedes shell building in organisms [1], and warming waters can disrupt coral growth. In-situ photos can be used to evidence changes, but 2D photos are rarely sufficient to capture the extension and development in time and in a three-dimensional world. Generally, pictures taken from different angles and by different persons are required to capture a good 3D view, e.g. to reduce image distortion or to capture more details, but aligning and merging photos is a non-trivial and demanding task and sometimes it is even necessary to return to the field again.

*Correspondence to: Istituto di Scienza e Tecnologie dell'Informazione "A. Faedo" (ISTI) – CNR
Via G. Moruzzi, 1 – 56124, Pisa – Italy
E-mail: coro@isti.cnr.it

Prepared using cpeauth.cls [Version: 2010/05/13 v3.00]

Reconstructing a 3D scene from a set of photos is a powerful modern technology that operates the reverse process of flattening a 3D scene into a 2D image. Photogrammetry (i.e. estimating real measurements from photographs) has incorporated sophisticated algorithms for structure-from-motion that estimate three-dimensional structures from a sequence of images. These algorithms produce clouds of virtual points in 3D from the photos and reconstruct a polygonal mesh from this cloud, even attaching a texture made up of sections of the photos.

Photogrammetry now finds applications in a wide range of domains, including cinematography and entertainment [2, 3, 4], cultural heritage [5, 6, 7, 8], and many branches of science [9, 10, 11, 12, 13, 14, 15]. For example, it is used to recreate movie locations in videogames [2], to reconstruct areas filmed by drones [16], and it can be combined with smart software to guide users towards the best poses to achieve optimal reconstructions [17]. However, most applications require specialised and expensive hardware (e.g. graphic cards, multi-core processors, etc.) and software. Good quality free and open-source 3D reconstruction software has been developed in recent years (e.g. OpenMVG and PMVS [18, 4]), but its performance cannot equal commercial software without complex and expert parametrisation [19, 20, 21, 22]. This limits the usage of 3D reconstruction techniques to small, expert, and resourceful communities of practice. A complete workflow would also need to add sharing tools to collect photos from multiple users, and tools to represent and publish the reconstructed scenes through heterogeneous visualisation facilities, e.g. virtual reality devices, smart-phones, personal computers, etc. Current solutions address small communities and have met strong issues due to variable data quality, heterogeneous data licensing, and poor user engagement [23]. Open-source solutions to handle reconstructions of large collections of shared photos on the Internet have been proposed, but currently fail at producing satisfactory results in terms of completeness and robustness [24, 25]. A general-purpose 3D reconstruction software that is able to automatically manage both large and small photos collections has never been achieved [26], but automatic photos viewpoint estimation - a sub-process of 3D reconstruction workflows - has been successfully used to organise unstructured collections of photos from the Internet related to monuments, buildings, and complex scenes [27, 28, 29]. On the other hand, the re-use and publication of reconstructed models in social networks and virtual reality applications is gaining success, thanks to the robustness and maturity of online 3D and virtual reality visualisation libraries and to the compatibility of most VR-ready devices with the products of 3D reconstruction processes [30, 31, 32]. However, these online visualisation and sharing environments are not directly integrated with 3D reconstruction development environments.

In this paper, an integrated workflow is proposed where a collaborative online system is used to both reconstruct and publish a virtual reality (VR) scene, accessible via Web, from a collection of shared photos (Figure 1). The workflow creates 3D objects using a combination of state-of-the-art open-source software components, and releases the produced objects and Web application in order to enable users to add information (e.g. markers and annotations) and thus to publish a more complete Web VR scene. The workflow has the possibility to combine photos from different users. It is continuous, i.e. new photos can be added, and the VR scene can be refined by running the workflow again. The technological support to sharing, processing, and publication is provided by a distributed e-Infrastructure. Overall, our workflow overcomes the limitations of the reported state-of-the art solutions by having all the used technology integrated on the same platform - i.e. from social networking and sharing facilities to 3D reconstruction processes and VR scenes publication - while reducing the usage complexity of each step. It can be used in many domains and for many tasks, e.g. for reconstructing cultural heritage artefacts, agricultural growth, and digital surveys. Our solution offers a free to use and all-in-one alternative to other 3D scenes reconstruction algorithms (e.g. [33, 4, 7]) and automatic virtual reality environments generation systems (e.g. [34, 31]), while autonomously managing requirements of hardware, expertise in photogrammetry, automation, and performance. It complies with the Open

DOI: 10.1002/cpe

Science paradigm [35], as each step is reproducible and repeatable, and reusable in several domains, including outside of the host e-Infrastructure. This is thanks to the use of a representation standard for the services involved, simple HTTP interfaces, and management of computational provenance.

2. MATERIAL AND METHODS

2.1. E-Infrastructure and collaborative tools

An e-Infrastructure is a distributed computer system that fosters collaboration between users and can embed distributed and parallel processing systems to manage computationally intensive tasks. It is usually implemented as a network of hardware and software resources (e.g. Web services, machines, processors, databases etc.) that enable users residing at remote sites to collaborate, exchange information, and conduct experiments. In order to support the workflow described in this paper, the D4Science e-Infrastructure was used [36]. D4Science has low cost of maintenance and operation, and hosts a rich array of services supporting several application domains [37]. Examples of applications based on D4Science include (i) analyses in fisheries science and marine biodiversity for stock assessment and species distribution estimates [38, 39, 40, 41], (ii) producing datasets and time series forecasts for climate change and environmental science studies [42, 43], (iii) processing big data for social mining [44], and (iv) building semantic networks for cultural heritage [45]. Further, D4Science supports the creation of Virtual Research Environments (VREs), i.e. Web-based, domain-oriented environments that support collaboration between groups of users focussing on the same domain of interest. After subscribing to the e-Infrastructure portal*, users are granted access to an online Workspace area, i.e. a virtual online file system where files can be uploaded and folders can be created and shared with other subscribed users. Users can ask access to VREs offering services and Web interfaces they find interesting, or that are related to a project they are involved in. For example, the workflow described in this paper was offered to the users of a public-access VRE named ScalableDataMining†, containing Web applications offering processing and visualisation tools for data scientists.

The D4Science Workspace builds upon a high-availability distributed storage system hosted by the e-Infrastructure and based on state-of-the-art technology [46] and offers an HTTP-REST interface for usage by other services‡. The Workspace is the main tool to support images sharing: Users can share folders to develop a repository of images of a particular object or environment. This folder can be also shared with all members of a VRE automatically, so that new subscribers would inherit the photos folder. A folder on the Workspace can be used as input to the computational services of the VRE. Computational outputs are automatically saved on a user's private Workspace and can be shared with other users again. The Workspace is also coupled with social networking facilities [37] that allow setting an automatic notification for new files added to a shared folder, and support (i) direct messaging between VRE users, (ii) news posting, and (iii) invitation of new users to join a VRE.

D4Science automatically manages security, accounting, and quota in order to monitor use of the storage and computational resources in a VRE. The D4Science terms of use, one of the first examples of FAIR-driven e-Infrastructure policies, make each user responsible for the content (s)he publishes, which applies also to the workflow here presented. The D4Science security and accounting services not only monitor the user's publications and help tracing inappropriate content, but also embed relevant attribution, provenance and quality metadata to both ingested data, algorithms, and generated output in a cloud platform.

*Publicly accessible after free registration at https://services.d4science.org

†Accessible after free registration at https://services.d4science.org/group/scalabledatamining/

‡https://wiki.gcube-system.org/gcube/Home_Library_REST_API

DOI: 10.1002/cpe

2.2. Cloud computing platform

The D4Science e-Infrastructure hosts a cloud computing platform named DataMiner [47, 48], an open-source system developed to meet < Science criteria of re-usability, reproducibility, and repeatability of experiments. It relies on the Web Processing Service standard (WPS, [49]) to represent processes. The complete set of input data, parameters, and output data (i.e. the computational provenance) is saved on the Workspace at the end of each computation, under the Prov-O XML format [50]. Each computational job can be parallelised for execution on multiple virtual cores of one machine. By combining computing requests distribution across machines with parallel processing on one machine, DataMiner is able to process Big Data, with support for the sharing of results and provenance.

DataMiner generates automatically Web GUIs for the hosted algorithms, through an intelligent interpretation of the WPS processes description. These GUIs allow users to select data from the D4Science Workspace and to use in calculations. DataMiner currently hosts about 400 algorithms provided by different communities of practice working in the D4Science VREs.

DataMiner is used for 3D reconstructions using a cluster of 15 machines with Ubuntu 16.04.4 LTS x86 64 operating system, 16 virtual cores, 32 GB of RAM and 100 GB of disk space, and of one additional machine with 64 GB RAM mounting an NVIDIA Titan XP 12GB-G5X graphics card. These machines are hosted in data centres of the National Research Council of Italy and of the Italian Network of the University and Research (GARR), and a load balancer distributes requests uniformly across machines.

2.3. 3D reconstruction pipeline

A 3D reconstruction process (*pipeline*[*]) was implemented to manage heterogeneous types of multi-image 3D reconstruction cases with no parametrisation options for the final user. This process was published as a Web service and an interface was provided to make it usable by the general public without pre-requisite technical knowledge on photogrammetry. These targeted cases covered images collections with (i) low to high resolution, (ii) small to large number, and (iii) focus either on small objects or on large environments. Our pipeline requires a set of images packaged in a ZIP file as input, which is generated from a D4science Workspace folder. The output is a compressed ZIP file containing (i) one cloud of 3D points estimated from the photos, in PLY file format, (ii) one reconstructed untextured mesh, in OBJ file format, (iv) the textured mesh, in OBJ format, along with texture images in JPG format, and (v) metadata indicating the files contents, the number of faces and points reconstructed, the position of a camera at the estimated central point of view of the scene, and the barycentre of the mesh.

The core of our pipeline combines open-source software components and libraries, i.e. OpenMVG [18], OpenMVS [51], Multi-View Environment (MVE) [52], and MVS-Texturing [53]. Our process automatically selects the best available software and differentiates its parametrisation depending on input characteristics. Our pipeline was tuned using a corpus of 100 uses cases (including those reported in Section 3.1) collected among the D4Science VREs, with heterogeneous subjects, images resolutions, and numbers of images. Eventually, the best association between input characteristics and reconstruction software and parametrisation was found. OpenMVG and OpenMVS were used as one sequence of tools, because OpenMVG can extract structure-from-motion by analysing photos and OpenMVS can work with its output to build the points cloud, and to reconstruct, refine, and texture the mesh. Likewise, MVE and MVS-texturing were sequenced together because MVE supports operations from structure-from-motion extraction to mesh reconstruction, and MVS-texturing is able to texturize this mesh. MVE+MVS-texturing is generally faster

[*]We will use the term pipeline to distinguish the 3D reconstruction process from our entire collaborative workflow.

DOI: 10.1002/cpe

than OpenMVG+OpenMVS and can obtain qualitatively comparable results on cases with many high-resolution images, but has worse performance otherwise. On the other hand, the reconstruction quality of the OpenMVG+OpenMVS concatenation strongly depends on its parametrisation. These pipelines were selected after an evaluation of the suitability of several free, open-source, and high-performance software components to support our target cases and automation level. Alternative software was evaluated on the capacity to automatically address even parts of the reconstruction process of the use cases with high quality, and included: Bundler [29], CMVS [54], PMVS [4], ColMap [26], MeshLab [55], Theia [56], VisualSFM [57], and BoofCV [58].

Our tuning operation resulted in the identification of three sub-pipelines that could alternatively reconstruct a sufficiently complete and detailed mesh. In the following, we report the non-default parameters used for each software:

1. OpenMVG+OpenMVS with brute force approach*
   (a) uses the L2 BruteForce algorithm for photos matching;
   (b) produces high-density points cloud;
   (c) uses all neighbour estimated views for depth-map estimation;
   (d) uses at least 2 matching images to start images fusion and common points estimation.
2. OpenMVG+OpenMVS with automatic matching approach†
   (a) uses an internal OpenMVG automatic selection process of the best suited algorithm for photos matching, which may use localised features instead of the global features used by the brute force approach. Available matching algorithms are: L2 BruteForce matching, L2 Approximate Nearest Neighbour matching, L2 Cascade Hashing matching, and L2 Cascade Hashing with precomputed hashed regions;
   (b) produces medium-density points cloud;
   (c) uses 4 neighbour views for depth-map estimation;
   (d) uses at least 3 images to start images fusion and common points estimation.
3. MVE+MVS-texturing‡. Uses standard MVE and MVS-texturing parametrisation and forces 'medium-density' for the reconstructed points clouds.

The three sub-pipelines were combined together into one overall pipeline (named *Open Mesh Reconstruction*, OMR), which executes the best suited sub-pipeline depending on input characteristics that were identified during the tuning operation:

1. If the average images resolutions is <= 7M pixels, use OpenMVG+OpenMVS with brute force approach.
2. Else, if the images set package size is <= 1.5GB, use OpenMVG+OpenMVS with automatic matching approach.
3. Else, use MVE+MVS-texturing.

Thus, the brute force approach is used for low-resolution images, where extracting and using the highest amount of information is fundamental. Instead, MVE+MVS-texturing is more convenient with many high-resolution images in terms of balance between quality and speed. In all other cases, OpenMVG+OpenMVS with automatic matching is the most appropriate sub-pipeline because of its better adaptability in terms of possible use

*The full script is available at http://data.d4science.org/NVByRTRJNHVDUk91czdsSkRIa0EvMDRNaVR3c1BETEVHbWJQNStIS0N6Yz0

†The full script is available at http://data.d4science.org/c2NxN3FNbUQwTWdQc3NicTZ1SkpGcit2YlpsQkdqQ1FHbWJQNStIS0N6Yz0

‡The full script is available at http://data.d4science.org/b3RjZURDdmhoZmF1czdsSkRIa0EvOTZ5aHZISXBWSzdHbWJQNStIS0N6Yz0

Prepared using cpeauth.cls
DOI: 10.1002/cpe

of localised features and different photos matching algorithms. Furthermore, it works on good resolution images (> 7M pixels) but keeps computational time short while producing good quality reproductions (as long as total input size is below 1.5 GB).

As a further step, OMR checks the files produced by the executed sub-pipeline, and transforms and harmonises them to always output the same types of files. Metadata about the number of produced points and faces, the central camera position, and the mesh barycentre are extracted from the data produced by the sub-pipelines and information is added as a text file into the output package. The produced output is saved by the DataMiner service on the user's Workspace in an automatically created folder, along with computational provenance information on the provided input, the produced output, and other metadata related to the user and the computational time.

Open Mesh Reconstruction was developed in JAVA and was published as a WPS process on DataMiner with an automatic Web interface associated*. In compliance with our goal, this interface does not require parametrisation nor expertise in photogrammetry.

2.4. Web application for virtual reality

DataMiner was also used to generate and publish Web applications to navigate and explore the objects and scenes produced by OMR (VRPublisher†). This builds upon a Web application template that can load and display both textured objects and clouds of 3D points. The template contains two standard HTML pages that connect to the textured mesh and to the points cloud respectively. These pages use the Three.js Javascript library [59] to prepare the scene and render the objects. Three.js uses the Web Graphics Library (WebGL), compatible with most Web browsers without requiring installation of additional plug-ins, which renders scenes using the graphics card of the visualisation device. The complex operations behind this rendering engine (e.g. calculating light reflections, shading, texturing, object relative positioning, etc.) are 'hidden' by the library to our applications and are described by other works [60, 61]. Three.js allows adding navigation controls and setting scene's lights and camera, and enables visualisation and interaction through virtual reality devices. A VR-ready device opening a Web application produced by VRPublisher projects the user inside the scene. On smart-phones, the applications can be visualised through the Google Cardboard, where head movements correspond to camera rotations and a bluetooth controller can be used for navigation. Other supported devices (through Three.js compliance) are Oculus Rift and HTC Vive.

The output of OMR is the input of VRPublisher. The process raises an alert if the mesh has more than 100,000 faces because visualization may then exceed target device requirements. VRPublisher processes and wraps the points cloud and the textured mesh files into a Web application containing configurable scenes parameters and objects, i.e (i) a uniform background light and one soft bullseye light, pointing to the object barycentre by default, (ii) Phong shading to enhance lights reflection quality, (iii) one camera placed by default at the central point of view estimated by OMR, which points at the object's barycentre with a 50 frustum vertical field of view. After wrapping objects in the scene, the Web application is packaged as a ZIP file and is transferred to one among a balanced set of Apache servers [62] hosted by D4Science. To complete the process, the Apache server publishes the Web application and assigns a unique URL.

In summary, the overall output of VRPublisher is made up of (i) one public link to a navigable virtual scene visualising the reconstructed textured mesh, (ii) one link to a navigable virtual scene visualising the points cloud, (iii) one ZIP package containing

*Freely accessible and usable in the ScalableDataMining D4Science VRE at https://services.d4science.org/group/scalabledatamining/data-miner?OperatorId=org.gcube.dataanalysis.wps.statisticalmanager.synchserver.mappedclasses.transducerers.OPEN_MESH_RECONSTRUCTOR

†Accessible in the ScalableDataMining VRE at https://services.d4science.org/group/scalabledatamining/data-miner?OperatorId=org.gcube.dataanalysis.wps.statisticalmanager.synchserver.mappedclasses.transducerers.VRPUBLISHER

DOI: 10.1002/cpe

the Web application source code. The source code is returned to the user to allow for customisation through the modification of the scene's parameters. Another DataMiner process allows publishing modified Web applications directly on the D4Science Apache servers (WebAppPublisher*).

2.5. Overall workflow

The overall workflow proposed in this paper combines together all the components described so far: A folder on the D4Science Workspace is shared between a number of users and is used as endpoint to collect photos of a certain object. One of the users starts the 3D reconstruction pipeline through the related DataMiner Web interface, indicating the shared photos folder as input. The produced 3D reconstruction object is possibly shared again with the other users and post-processed in order to add details, annotations, or new objects and thus to build a more complete 3D scene. Finally, the 3D object (or the enriched scene) is passed as input to the VRPublisher service through the DataMiner interface in order to publish two VR Web applications that display the points cloud and the textured reconstructed mesh respectively. These Web applications can be customised through their source code and can be published again if adjustments are required. The links to these applications can be either shared between the users or distributed through other social networking channels as publicly accessible links. Automatic sharing of all workflow steps can be enable by directly sharing the Workspace folder where DataMiner saves the outputs of the computations. With this configuration, every user would be able to start the 3D reconstruction or the VR publication processes at any time, based on the data possibly produced by the other users. The workflow could be executed as soon as new photos were shared, in order to continuously refine the 3D reconstructions and VR scenes.

3. RESULTS

In this section, the performance of the Open Mesh Reconstruction process are compared with those of a commercial software and of another open-source solution. This highlights that the balance between computational speed and quality in our process is satisfying although it requires no parametrisation. Other benefits and possible usages of our workflow are demonstrated by means of three practical use cases that involve it in marine biodiversity conservation projects.

3.1. Performance

The performance of OMR was compared to two other 3D reconstruction applications: the Agisoft Photoscan†, a commercial high-quality software that addresses the same reconstruction cases and automation level of our pipeline, and MVE+MVS Texturing (indicated simply as MVE), one of the components of our OMR. OpenMVG and OpenMVS were excluded as a standalone software because their usage with default configuration could not produce results in most of our test cases.

Photoscan has a number of parameters‡, but the most relevant in our test cases were: (i) The accuracy of the photos matching algorithm (High/Medium), (ii) the resolution of the target points cloud (Ultra/High/Medium), and (iii) the filter to use on the points cloud

*Accessible in the ScalableDataMining VRE at https://services.d4science.org/group/scalabledatamining/data-miner?OperatorId=org.gcube.dataanalysis.wps.statisticalmanager.synchserver.mappedclasses.transducerers.WEB_APP_PUBLISHER

†www.agisoft.com

‡For the complete list refer to the software manual http://www.agisoft.com/pdf/photoscan-pro_1_4_en.pdf

Prepared using cpeauth.cls
DOI: 10.1002/cpe

in the mesh reconstruction phase (Aggressive/No filtering). The Photoscan results were reported only for the parametrisation producing the best results.

As test cases, 11 sets of photos* with growing size and heterogeneous difficulty for the mesh reconstruction processes were used (Table I and Figure 2). Some cases (ET, Kermit, Castle) are common benchmarks for photogrammetry software. These cases involve few low-resolution images, and one case rotated of 90° in order to verify that reconstruction is independent on rotation. Two cases (Person and Dog) involve slightly moving objects, which represent particularly hard cases because 3D reconstruction algorithms cannot work with moving objects. The Compass and Skeleton cases contain few images with high resolution, but in Skeleton the object is larger. This case was provided by a D4Science VRE of archaeologists focussing on cultural heritage studies. The Colony, Wreck, and Reef cases were provided by Marche Polytechnic University and aim to test effectiveness at reconstructing underwater objects with increasing size and complexity, i.e. (i) a coral with thin structure, (ii) a shipwreck in murky waters, and (iv) a large coral reef area.

A first performance comparison was made on computation time (Figure 3-a and Table II-a). OMR time was reported using GPU and CPUs separately to highlight that GPU reduces average computation time with 21.3%. The hardware configuration for GPU and CPUs was the one reported in Section 2.2. Photoscan and MVE performance were measured on GPU only. Gaps in the lines are visible for MVE where it failed at reconstructing in some of the cases. Overall, an increasing trend in computation time is observable across the use cases, with a 'flat' segment around those with medium difficulty (i.e. from Castle to Wreck), which OMR manages using OpenMVG+OpenMVS with automatic matching. Instead, OMS uses MVE+MVE Texturing in the Reef case. In the other cases, OMR used OpenMVG+OpenMVS with brute force approach. Increasing trends also show in the numbers of points and faces (Figures 3-b-c and Table II-b-c), with Photoscan producing significantly fewer points and faces on large inputs. The ratio between processing time and input size (Figure 3-d and Table II-d) indicates that Photoscan requires increasing processing times because it optimises points and faces. Also, Photoscan tends to maintain the ratio between the number of faces and points constant, with a hockey stick trend observable in our test cases (Figure 3-e and Table II-e). As input size increases, OMR tends to produce an equal number of points and faces. After 1.5 GB of input size, OMR uses MVE+MVS Texturing exclusively because with this size and high resolution images the reconstruction quality of this pipeline increases and the computational time is contained [52].

The reconstruction effectiveness also depends on the photographed object. This aspect was explored through a qualitative performance assessment by three human evaluators, external to this experiment, who assigned a quality label to each reconstruction among High, Medium, and Low. In particular, the evaluators judged 4 aspects: (i) Completeness of the reconstructed scene, (ii) quality of the details, (iii) recognizability of the scene, (iv) realism (i.e. suitability of use in a VR scene). An overall quality assessment was reported for each reconstruction as the label most assigned by the evaluators across all aspects (Figure 4-a and Table II-f). The most assigned labels for each aspect are reported in Figures 4-b-e and Tables II-g-l. OMR was given the highest overall quality evaluation and Photoscan had the best balance between High and Medium labels. Photoscan and OMR differ notably on moving objects reconstruction: Photoscan reconstructs the Person case better than OMR, because it reconstructs most of the person but also part of the room (i.e. it is completer). However, OMR has better performance in the Dog case, where the object moves more. In the Colony case, the Photoscan reconstruction is smaller and the details of the object are mostly missing, whereas OMR results in full reconstruction. In the Wreck case, the object

*Available at
http://data.d4science.org/workspace-explorer-app?folderId=
eW43dDVjZktEVWZlbXBQZjUwbnM4bkZWT2lhNDBtekFrMWRDZ0NVUkFyaDgwcFNsTnlJeFRtKzFZQmIrWkxxSA

DOI: 10.1002/cpe

is completely reconstructed by all workflows except for MVE, which finds matches only between a small subset of images and reconstructs just a part of the wreck, although with high quality. Finally, in the Reef case all workflows produce high quality results, but no scene is complete because parts of the area are missing in all reconstructions.

3.2. Use cases

3.2.1. Underwater surveys

The Green Bubbles* European ITN project promotes sustainable development of scuba diving and conservation of underwater habitat through the engagement of scuba divers. This project uses underwater photogrammetry as a flexible and reliable technique for high resolution benthic habitat mapping [63] and aims at developing new products for scuba divers suitable for citizen science programs [64]. In order to test our 3D reconstruction pipeline, Green Bubbles provided more than 3000 photos taken on different days covering partially overlapping coral reef areas in Indonesia. These photos where uploaded on the D4Science Workspace and the 3D reconstruction pipeline produced an object representing an over 2000 square meters area (using MVE). To enhance reconstruction details, parts of the area - mapped with 10 sets of 300 photos - were reconstructed (where OMR used OpenMVG+OpenMVS with automatic matching) and the 10 reconstructions were merged with the overall reconstruction. Green Bubbles considered our final result sufficient to survey the coral reef's structural changes over time through the comparison of 3D reconstructions.

3.2.2. Ecological monitoring

The MERCES† European project aims at restoring underwater habitats in the Mediterranean Sea by transplanting several benthic species. In this context, monitoring organisms' growth is paramount for addressing the success of restoration actions but it can be challenging with slow growing species like gorgonian corals. Thus, photogrammetric surveys were performed by executing our workflow on 10 transplanted colonies of *Eunicella singularis* gorgonian at Gallinara island (North-West Italian Tyrrhenian Sea), and these colonies were reproduced through 3D scaled virtual representations. The used image datasets contained from 50 to 100 high-resolution images. The performances of OMG and Photoscan were compared in processing the imagery. OMR was able to reconstruct the 3D coral structures completely in 9 cases and Photoscan in 6 cases (Figure 5 compares the results on one example). Furthermore, the average ratio between the number of cloud points of the coral and of its reconstructed surrounding area was 18% for OMR and 27% for Photoscan, which indicates that OMR reconstructs more background than Photoscan. The OMR results allowed for fine measurement (<0.5 cm) of the corals' lengths and were thus suited to calculate growth over time. As an additional feature, the photographic mesh texture, visualised through a VR scene‡, proved useful for assessing health status by showing the presence and extension of infected and damaged portions.

3.2.3. Education

The Green Bubbles project, together with Universitá Politecnica delle Marche, Divers Alert Network Europe§, the Professional Association of Diving Instructors¶ and Project AWARE‖ promote a postgraduate course for research divers**. The course trainers organise underwater surveys to explain scuba-diving for conservation biology and sustainable

*www.greenbubbles.eu
†www.merces-project.eu
‡One example is available at http://access.d4science.org/Coral/
§www.daneurope.org
¶www.padi.com
‖www.projectaware.org
**http://www.univpm.it/Entra/Corso_di_perfezionamento_ed_aggiornamento_professionale

DOI: 10.1002/cpe

tourism. In one of these surveys in Malta*, students took underwater pictures of a 60 m long shipwreck and collected a total of 500 photos during a single dive. Each student covered a small portion of the shipwreck. After the dive, the photos were collected on the D4Science Workspace and our workflow was used to reconstruct and visualise the complete shipwreck. This highlighted to the students the potential of our technology and its possible usage in communication and dissemination.

4. DISCUSSION AND CONCLUSIONS

In this paper, a workflow has been presented that enables collaboration to build VR representations of photographed objects. Our workflow takes full advantage of shared pictures and makes its users overcome common hardware issues by using an e-Infrastructure, an online storage system, and a cloud computing platform. The advanced automation of the workflow allows also users that are not experts of photogrammetry and Web applications to collaborate and produce results. Computational resources are cloud based and shared among different communities organised into Virtual Research Environments, which reduces maintenance and provisioning costs and allows even to offer a free to use solution.

The products produced by our workflow can be all re-managed and shared by users before and after the publication of the virtual reality scenes. The performance of our Open Mesh Reconstruction process are comparable with a commercial software on a number of test cases with full process automation and no parametrisation. Practical benefits were highlighted through use cases in marine science with both research and educational purposes, where our workflow was found useful for its effectiveness and for not adding costs. Applications can be extended also to other domains, which may require specific tuning or enhancement of OMR. These applications are being evaluated in D4Science VREs related to archaeology, agriculture, and citizen science in European projects†.

The DataMiner computational platform exposes OMR and VRPublisher as WPS services. This implies that their input and output data are described in a human- and machine-understandable XML description and the WPS can be invoked via simple HTTP-GET or POST calls. By simply pasting a HTTP query string in a Web browser or through any programming language, it is possible to execute, repeat, and reproduce an experiment. WPS calls can be easily (often natively) called by workflow management engines (e.g. Galaxy, [65], KNIME, [66], etc.) and thus our processes can be used to produce new automatic workflows. Overall, WPS facilitates the use of our processes in applications external to the e-Infrastructure, e.g. in Web sites and third party applications. This feature makes the services appealing because it makes technology and hardware seamlessly and easily available. An external user or application connected to the WPS services is requested to identify itself through a security token in the HTTP request. This token enables security, accounting, and quota management for incoming requests and allows D4Science to flexibly assign higher performance resources to a group of users (when paying for these resources). Finally, saving metadata after the execution of the workflow enables features as (i) consulting previous versions of the reconstructions, (ii) executing the workflow of another user (repeatability), (iii) making other users reproduce a 3D virtual scene after slightly changing the mesh or the photos (reproducibility). In summary, we successfully developed our workflow to be compliant with Open Science in terms of knowledge sharing, production of new knowledge, collaborative experimentation, and repeatability, reproducibility, and re-usability of the products.

*https://divewise.com.mt/courses/start-scuba/padi-open-water-diver.php
†www.parthenos-project.eu, www.plus.aginfra.eu, and sobigdata.eu

DOI: 10.1002/cpe

ACKNOWLEDGMENTS

We gratefully acknowledge the support of NVIDIA Corporation with the donation of the Titan XP GPU used for this research. We thank the Green Bubbles community (Marie Sklodowska-Curie grant agreement No 643712) the MERCES project (Horizon 2020 research and innovation programme grant agreement No 689518) and Universitá Politecnica delle Marche for providing test material and use cases. Special thanks to Dr. Jacopo Caroni for collaborating in the data collection phase.

References

1. Ries JB. Oceanography: A sea butterfly flaps its wings. Nature Geoscience 2012; 5(12):845.
2. Statham N. Use of photogrammetry in video games: A historical overview. Games and Culture 2018; 1:1–19.
3. PixPro Ltd. Photogrammetry: From Movies to Software Solutions 2018. https://geo-matching.com/content/photogrammetry-from-movies-to-software-solutions.
4. Furukawa Y, Ponce J. Accurate, dense, and robust multiview stereopsis. IEEE transactions on pattern analysis and machine intelligence 2010; 32(8):1362–1376.
5. Melón V, Rodríguez Miranda Á, Martínez Lázaro R, Pérez Vidiella P, Uceda Queirós S, Lopetegi Galarraga A. New metric products, movies and 3d models from old stereopairs and their application to the in situ palaeontological site of ambrona. Online publication http://hdl.handle.net/10810/24751 2017; 1:1–16.
6. Georgopoulos A, Oikonomou C, Adamopoulos E, Stathopoulou E. Evaluating unmanned aerial platforms for cultural heritage large scale mapping. International Archives of the Photogrammetry, Remote Sensing & Spatial Information Sciences 2016; 41:1–8.
7. Koutsoudis A, Vidmar B, Ioannakis G, Arnaoutoglou F, Pavlidis G, Chamzas C. Multi-image 3d reconstruction data evaluation. Journal of Cultural Heritage 2014; 15(1):73–79.
8. Roncella R, Re C, Forlani G. Performance evaluation of a structure and motion strategy in architecture and cultural heritage. Int. Archives of Photogrammetry, Remote Sensing and Spatial Information Sciences 2011; 38(5/W16):285–292.
9. Palma M, Rivas Casado M, Pantaleo U, Pavoni G, Pica D, Cerrano C. Sfm-based method to assess gorgonian forests (paramuricea clavata (cnidaria, octocorallia)). Remote Sensing 2018; 10(7), doi:10.3390/rs10071154. URL http://www.mdpi.com/2072-4292/10/7/1154.
10. Pavoni G, Palma M, Callieri M, Dellepiane M, Cerrano C, Pantaleo U, Scopigno R. Quasi-orthorectified projection for the measurement of red gorgonian colonies. ISPRS - International Archives of the Photogrammetry, Remote Sensing and Spatial Information Sciences 2018; XLII-2:853–860, doi:10.5194/isprs-archives-XLII-2-853-2018.
11. Law K, West G, Murray P, Lynch C. 3-d advanced gas-cooled nuclear reactor fuel channel reconstruction using structure-from-motion. 10th International Topical Meeting on Nuclear Plant Instrumentation, Control and Human Machine Interface Technologies, 2017.
12. Piton G, Recking A, Le Coz J, Bellot H, Hauet A, Jodeau M. Reconstructing depth-averaged open-channel flows using image velocimetry and photogrammetry. Water Resources Research 2018; 54(6):4164–4179.
13. Johnson-Roberson M, Pizarro O, Williams SB, Mahon I. Generation and visualization of large-scale three-dimensional reconstructions from underwater robotic surveys. Journal of Field Robotics 2010; 27(1):21–51.
14. Fulton C, Viduka A, Hutchison A, Hollick J, Woods A, Sewell D, Manning S. Use of photogrammetry for non-disturbance underwater survey: An analysis of in situ stone anchors. Advances in Archaeological Practice 2016; 4(1):17–30.
15. Akbarzadeh A, Frahm JM, Mordohai P, Clipp B, Engels C, Gallup D, Merrell P, Phelps M, Sinha S, Talton B, et al.. Towards urban 3d reconstruction from video. 3D Data Processing, Visualization, and Transmission, Third International Symposium on, IEEE, 2006; 1–8.
16. Alizadehashrafi B, Abdul-Rahman A. Using affordable data capturing devices for automatic 3d city modelling. ISPRS-International Archives of the Photogrammetry, Remote Sensing and Spatial Information Sciences 2017; 1:9–13.
17. Burton N, Nguyen V. Curated photogrammetry Apr 26 2018. US Patent App. 15/621,944.
18. Moulon P, Monasse P, Perrot R, Marlet R. Openmvg: Open multiple view geometry. International Workshop on Reproducible Research in Pattern Recognition, Springer, 2016; 60–74.
19. Mlambo R, Woodhouse IH, Gerard F, Anderson K. Structure from motion (sfm) photogrammetry with drone data: a low cost method for monitoring greenhouse gas emissions from forests in developing countries. Forests 2017; 8(3):68.
20. Remondino F, Spera MG, Nocerino E, Menna F, Nex F. State of the art in high density image matching. The Photogrammetric Record 2014; 29(146):144–166.
21. Koutsoudis A, Vidmar B, Arnaoutoglou F. Performance evaluation of a multi-image 3d reconstruction software on a low-feature artefact. Journal of Archaeological Science 2013; 40(12):4450–4456.
22. James M, Robson S. Straightforward reconstruction of 3d surfaces and topography with a camera: Accuracy and geoscience application. Journal of Geophysical Research: Earth Surface 2012; 117(F3).

DOI: 10.1002/cpe

23. Johnson P, Ricker B, Harrison S. Volunteered drone imagery: challenges and constraints to the development of an open shared image repository. HICSS '17 Proceedings of the 50th Hawaii International Conference on System Sciences, 2017; 1995–2004.
24. Frahm JM, Fite-Georgel P, Gallup D, Johnson T, Raguram R, Wu C, Jen YH, Dunn E, Clipp B, Lazebnik S, et al.. Building rome on a cloudless day. European Conference on Computer Vision, Springer, 2010; 368–381.
25. Heinly J, Schonberger JL, Dunn E, Frahm JM. Reconstructing the world* in six days*(as captured by the yahoo 100 million image dataset). Proceedings of the IEEE Conference on Computer Vision and Pattern Recognition, 2015; 3287–3295.
26. Schonberger JL, Frahm JM. Structure-from-motion revisited. Proceedings of the IEEE Conference on Computer Vision and Pattern Recognition, 2016; 4104–4113.
27. Schönberger JL, Zheng E, Frahm JM, Pollefeys M. Pixelwise view selection for unstructured multi-view stereo. European Conference on Computer Vision, Springer, 2016; 501–518.
28. Martin-Brualla R, Gallup D, Seitz SM. Time-lapse mining from internet photos. ACM Transactions on Graphics (TOG) 2015; 34(4):62.
29. Snavely N, Seitz SM, Szeliski R. Photo tourism: exploring photo collections in 3d. ACM transactions on graphics (TOG), vol. 25, ACM, 2006; 835–846.
30. Sketchfab. Sketchfab: the world's largest platform to publish, share, and discover 3D content on web, mobile, AR, and VR 2018. www.sketchfab.com.
31. Scopigno R, Callieri M, Dellepiane M, Ponchio F, Potenziani M. Delivering and using 3d models on the web: are we ready? Virtual Archaeology Review 2017; 8(17):1–9.
32. Fukuda T, Nada H, Adachi H, Shimizu S, Takei C, Sato Y, Yabuki N, Motamedi A. Integration of a structure from motion into virtual and augmented reality for architectural and urban simulation. International Conference on Computer-Aided Architectural Design Futures, Springer, 2017; 60–77.
33. Seitz SM, Curless B, Diebel J, Scharstein D, Szeliski R. A comparison and evaluation of multi-view stereo reconstruction algorithms. Computer vision and pattern recognition, 2006 IEEE Computer Society Conference on, vol. 1, IEEE, 2006; 519–528.
34. Olshannikova E, Ometov A, Koucheryavy Y, Olsson T. Visualizing big data with augmented and virtual reality: challenges and research agenda. Journal of Big Data 2015; 2(1):22.
35. Hey T, Tansley S, Tolle KM, et al.. The fourth paradigm: data-intensive scientific discovery, vol. 1. Microsoft research Redmond, WA, 2009.
36. Candela L, Castelli D, Pagano P. D4science: an e-infrastructure for supporting virtual research environments. IRCDL, 2009; 166–169.
37. Assante M, Candela L, Castelli D, Coro G, Lelii L, Pagano P. Virtual research environments as-a-service by gcube. PeerJ Preprints 2016; 2016(10):1–8.
38. Coro G, Vilas LG, Magliozzi C, Ellenbroek A, Scarponi P, Pagano P. Forecasting the ongoing invasion of lagocephalus sceleratus in the mediterranean sea. Ecological Modelling 2018; 371:37–49.
39. Candela L, Castelli D, Coro G, Pagano P, Sinibaldi F. Species distribution modeling in the cloud. Concurrency and Computation: Practice and Experience 2016; 28(4):1056–1079.
40. Coro G, Webb TJ, Appeltans W, Bailly N, Cattrijsse A, Pagano P. Classifying degrees of species commonness: North sea fish as a case study. Ecological modelling 2015; 312:272–280.
41. Coro G, Large S, Magliozzi C, Pagano P. Analysing and forecasting fisheries time series: purse seine in indian ocean as a case study. ICES Journal of Marine Science 2016; 73(10):2552–2571.
42. Trumpy E, Coro G, Manzella A, Pagano P, Castelli D, Calcagno P, Nador A, Bragasson T, Grellet S, Siddiqi G. Building a european geothermal information network using a distributed e-infrastructure. International Journal of Digital Earth 2016; 9(5):499–519.
43. Coro G, Magliozzi C, Ellenbroek A, Kaschner K, Pagano P. Automatic classification of climate change effects on marine species distributions in 2050 using the aquamaps model. Environmental and ecological statistics 2016; 23(1):155–180.
44. Grossi V, Rapisarda B, Giannotti F, Pedreschi D. Data science at sobigdata: the european research infrastructure for social mining and big data analytics. International Journal of Data Science and Analytics 2018; 1:1–12.
45. Blanke T, Hedges M. Scholarly primitives: Building institutional infrastructure for humanities e-science. Future Generation Computer Systems 2013; 29(2):654–661.
46. Banker K. MongoDB in action. Manning Publications Co., 2011.
47. Coro G, Candela L, Pagano P, Italiano A, Liccardo L. Parallelizing the execution of native data mining algorithms for computational biology. Concurrency and Computation: Practice and Experience 2015; 27(17):4630–4644.
48. Coro G, Panichi G, Scarponi P, Pagano P. Cloud computing in a distributed e-infrastructure using the web processing service standard. Concurrency and Computation: Practice and Experience 2017; 29(18).
49. Schut P, Whiteside A. Openggis® web processing service, version 1.0. 0, ogc 05-007r7, open geospatial consortium. Inc 2007; 87.
50. Belhajjame K, Cheney J, Corsar D, Garijo D, Soiland-Reyes S, Zednik S, Zhao J. Prov-o: The prov ontology. W3C Working Draft 2012; .
51. Cernea D. OpenMVS: open multiple view stereovision 2015. https://github.com/cdcseacave/openMVS/.
52. Fuhrmann S, Langguth F, Goesele M. Mve-a multi-view reconstruction environment. GCH, 2014; 11–18.
53. Waechter M, Moehrle N, Goesele M. Let there be color! large-scale texturing of 3d reconstructions. European Conference on Computer Vision, Springer, 2014; 836–850.

DOI: 10.1002/cpe

54. Furukawa Y, Curless B, Seitz SM, Szeliski R. Towards internet-scale multi-view stereo. Computer Vision and Pattern Recognition (CVPR), 2010 IEEE Conference on, IEEE, 2010; 1434–1441.
55. Cignoni P, Callieri M, Corsini M, Dellepiane M, Ganovelli F, Ranzuglia G. Meshlab: an open-source mesh processing tool. Eurographics Italian Chapter Conference, vol. 2008, 2008; 129–136.
56. Sweeney C, Hollerer T, Turk M. Theia: A fast and scalable structure-from-motion library. Proceedings of the 23rd ACM international conference on Multimedia, ACM, 2015; 693–696.
57. Wu C, et al.. Visualsfm: A visual structure from motion system (2011). Online publication http://www.cs.washington.edu/homes/ccwu/vsfm 2011; 14.
58. Abeles P. BoofCV 2018. http://boofcv.org.
59. Cabello R. three. js—javascript 3d library 2016. https://threejs.org.
60. Cozzi P. WebGL Insights 2015. CRC Press - online open publication http://www.webglinsights.com/.
61. Lengyel E. Mathematics for 3D game programming and computer graphics. Cengage Learning, 2012.
62. Fielding RT, Kaiser G. The apache http server project. IEEE Internet Computing 1997; 1(4):88–90.
63. Palma M, Rivas Casado M, Pantaleo U, Cerrano C. High Resolution Orthomosaics of African Coral Reefs: A Tool for Wide-Scale Benthic Monitoring. Remote Sensing 2017; 9(7).
64. Scaradozzi D, Zingaretti S, Panebianco L, Altepe C, Egi SM, Palma M, Pantaleo U, Ferraris D, Micheli F, et al.. Docuscooter: A novel robotics platform for marine citizen science. The 27th International Ocean and Polar Engineering Conference, International Society of Offshore and Polar Engineers, 2017.
65. Giardine B, Riemer C, Hardison RC, Burhans R, Elnitski L, Shah P, Zhang Y. Galaxy: a platform for interactive large-scale genome analysis. Genome Research 2005; 10(15):1451–1455.
66. Berthold MR, Cebron N, Dill F, Gabriel TR, Kötter T, Meinl T, Ohl P, Thiel K, Wiswedel B. Knime-the konstanz information miner: version 2.0 and beyond. AcM SIGKDD explorations Newsletter 2009; 11(1):26–31.

DOI: 10.1002/cpe

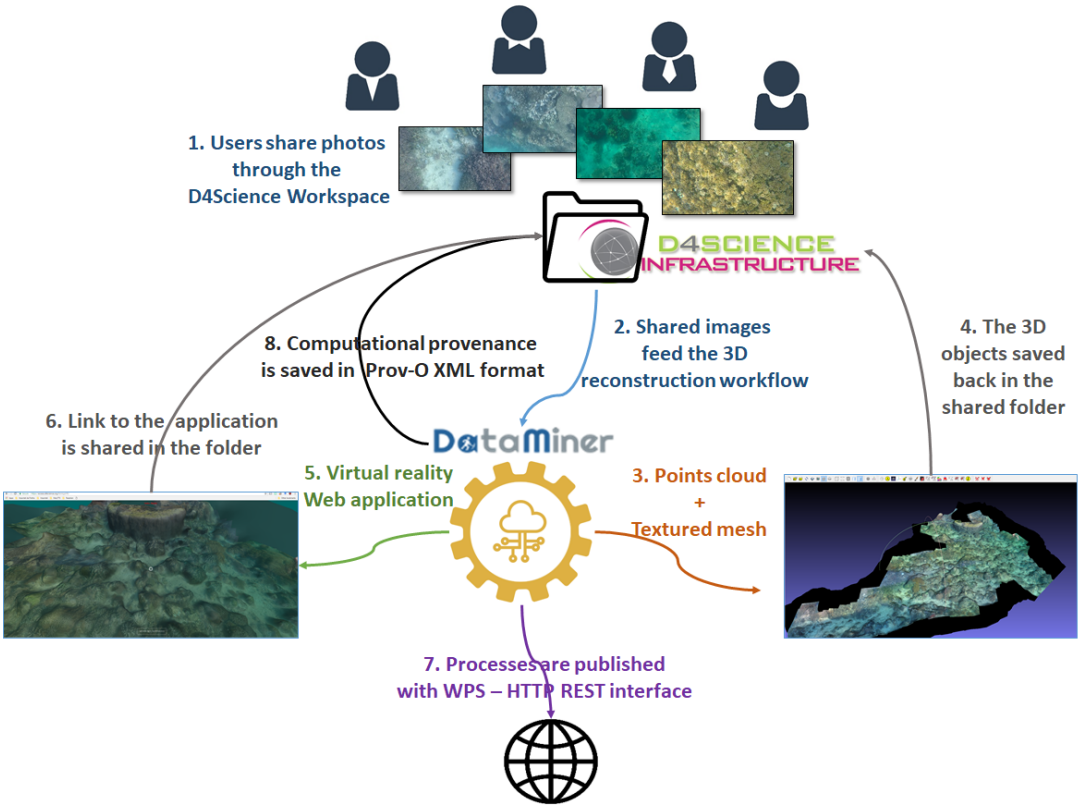

Figure 1. Representation of our workflow with the major eight operations highlighted.

DOI: 10.1002/cpe

Figure 2. Overview of the 3D reconstructions of our test cases by OMR, with wireframe view overlaid to the meshes to highlight faces sizes: (a) ET vertical, (b) ET horizontal, (c) Kermit, (d) Person, (e) Castle, (f) Compass, (g) Colony, (h) Dog, (i) Skeleton, (l) Wreck, (m) Reef.

DOI: 10.1002/cpe

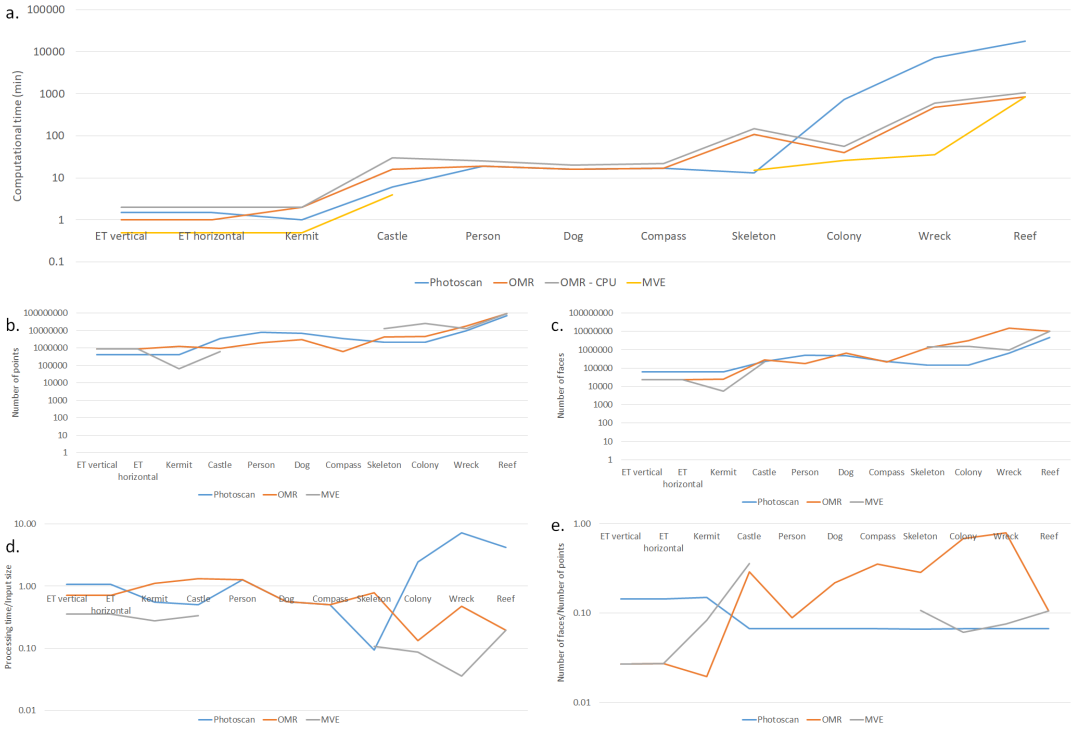

Figure 3. Comparison between the performance of Open Mesh Reconstruction - using alternatively NVIDIA Titan XP GPU (OMR) and 16 virtual CPUs (OMR-CPU) -, Agisoft Photoscan on GPU, and (iii) the Multi-View Environment+MVS-Texturing pipeline on GPU (MVE). The charts report (a) the computational time across our selected test cases, (b) the number of points in the produced dense clouds, (c) the number of faces of the reconstructed meshes, (d) the ratio between processing time and input size, and (e) the ratio between number of faces and points. The charts are all in logarithmic scale.

DOI: 10.1002/cpe

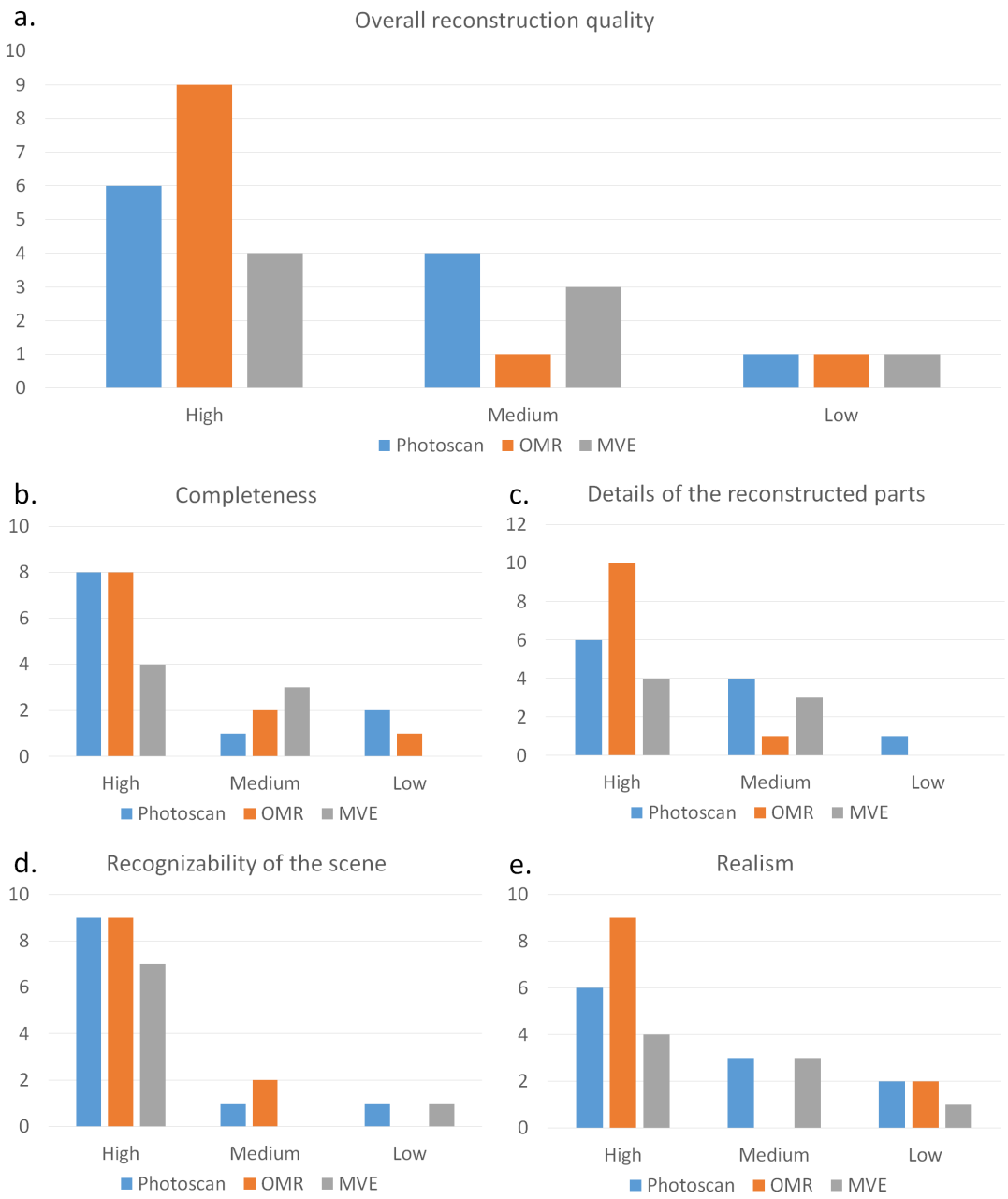

Figure 4. Comparison between Open Mesh Reconstruction (OMR), Agisoft Photoscan, and the Multi-View Environment+MVS-Texturing (MVE), in terms of (a) overall reconstruction quality across our test cases, (b) completeness of the reconstruction, (c) quality of the details of the reconstructed parts, (d) recognizability of the scene, (e) suitability of the product for a virtual reality scene (realism).

DOI: 10.1002/cpe

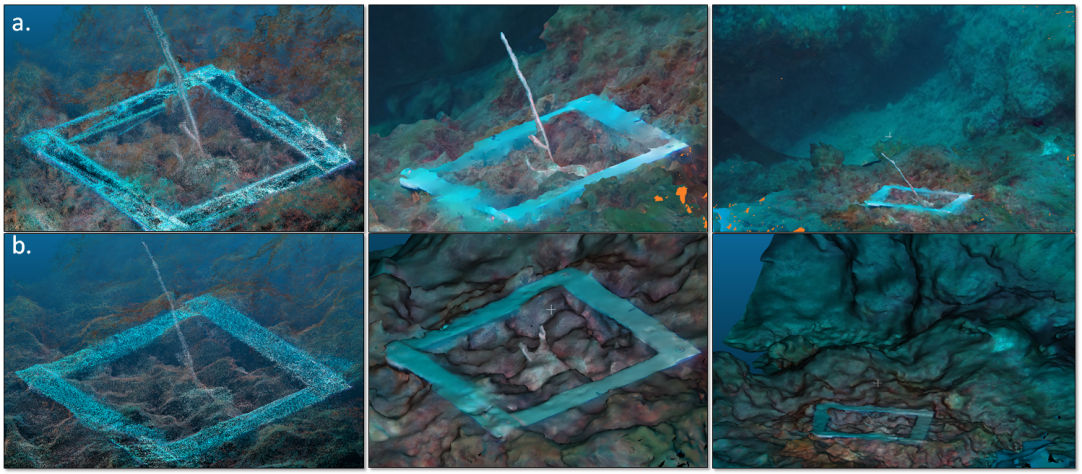

Figure 5. Reconstruction sequences of a coral, based on 98 photos taken by three divers. The sequences report the points clouds, the reconstructed objects, and the reconstructed scenes of (a) Open Mesh Reconstruction and (b) Agisoft Photoscan.

DOI: 10.1002/cpe

Use Case	Description	Size (MB)	Number of photos	Photos size	Camera	Photoscan best parameters
ET vertical	Few photos of a doll with no other object adjacent	1.4	9	640 x 480	Canon PowerShot A10	Matching accuracy: High; Points cloud quality: Ultra; Filtering: Aggressive
ET horizontal	Few photos of a doll with no other object adjacent - right rotated 90 deg.	1.4	9	640 x 480	Canon PowerShot A10	Matching accuracy: High; Points cloud quality: Ultra; Filtering: Aggressive;
Kermit	Few photos of a doll with other objects around the subject	1.8	14	640 x 480	Canon PowerShot A10	Matching accuracy: High; Points cloud quality: Medium; Filtering: Aggressive
Castle	Hi Resolution photos of a building facade	12	12	2832 x 2128	KODAK Z612 ZOOM DIGITAL CAMERA	Matching accuracy: Medium; Points cloud quality: Medium; Filtering: Moderate
Person	Full rotation around a person in a room	15	41	1600 x 1200	Canon PowerShot G9	Matching accuracy: High; Points cloud quality: Ultra; Filtering: Aggressive
Dog	Full rotation around a dog moving her head on a bed	28	10	2340 x 4160	LG-D855	Matching accuracy: High; Points cloud quality: Ultra; Filtering: No filtering
Compass	Full rotation around an object on a table	34	15	2341 x 4160	LG-D856	Matching accuracy: High; Points cloud quality: Ultra; Filtering: No filtering
Skeleton	Photos of a skeleton in archaeological site	139	20	3000 x 4496	NIKON D7100	Matching accuracy: High; Points cloud quality: Medium; Filtering: Aggressive
Colony	Photos of a very thin gorgonian transplanted coral surrounded by a metal-blue square marker at ground	300	79	4000 x 3000	GoPro HERO3+ Black Edition	Matching accuracy: High; Points cloud quality: Medium; Filtering: Aggressive
Wreck	Underwater photos of a ship wreck	1000	579	3000 x 2250	GoPro HERO3+ Black Edition	Matching accuracy: High; Points cloud quality: Medium; Filtering: Aggressive
Reef	Underwater photos of a coral reef	4300	3174	3000 x 2250	GoPro HERO3+ Black Edition	Matching accuracy: High; Points cloud quality: Medium; Filtering: Aggressive

Table I. Description of the test cases used in our performance comparison with indication of the input size, the number and the size of the photos, and the used camera. The last column reports the best parametrisation of Agisoft Photoscan for each case.

DOI: 10.1002/cpe

	ET vertical	ET horizontal	Kermit	Castle	Person	Dog	Compass	Skeleton	Colony	Wreck	Reef
	a. Processing time (min) (PT)										
Photoscan	1.5	1.5	1	6	19	16	17	13	730	7200	18000
OMR	1	1	2	16	19	16	17	110	40	480	840
OMR - CPU	2	2	2	30	25	20	22	150	57	600	1050
MVE	0.5	0.5	0.5	4	0	0	0	15	26	36	840
	b. Number of points in the cloud (NP)										
Photoscan	415148	415307	399311	3476041	7681742	6910916	3476041	2135960	2152256	9523136	71587298
OMR	879055	872055	1240647	953532	1995467	2993749	618777	4369309	4484631	18509857	93694414
MVE	877264	869968	65867	616131	-	-	-	13158752	24947008	13005672	93694414
	c. Number of faces in the reconstructed mesh (NF)										
Photoscan	59999	60000	60000	231735	512116	460726	231735	142186	143483	634875	4772481
OMR	23549	23758	24349	275151	176120	656217	219517	1250669	3047965	14557784	9950054
MVE	23598	23636	5474	220522	-	-	-	1404766	1524403	985944	9950054
	d. Ratio between processing time and input size (IS) : PT/IS										
Photoscan	1.07	1.07	0.56	0.50	1.27	0.57	0.50	0.09	2.43	7.20	4.19
OMR	0.71	0.71	1.11	1.33	1.27	0.57	0.50	0.79	0.13	0.48	0.20
MVE	0.36	0.36	0.28	0.33	0.00	0.00	0.00	0.11	0.09	0.04	0.20
	e. Ratio between the numbers of faces and points : NF/NP										
Photoscan	0.14	0.14	0.15	0.07	0.07	0.07	0.07	0.07	0.07	0.07	0.07
OMR	0.03	0.03	0.02	0.29	0.09	0.22	0.35	0.29	0.68	0.79	0.11
MVE	0.03	0.03	0.08	0.36	0.00	0.00	0.00	0.11	0.06	0.08	0.11
	f. Overall reconstruction quality										
Photoscan	High	High	High	Medium	Medium	Low	Medium	High	Medium	High	High
OMR	High	High	High	High	Low	Medium	High	High	High	High	High
MVE	High	High	Medium	Medium	NA	NA	NA	High	Medium	Low	High
	g. Completeness										
Photoscan	High	High	High	High	High	Low	High	High	Low	High	Medium
OMR	High	High	High	High	Low	Medium	High	High	High	High	Medium
MVE	High	High	Medium	High	NA	NA	NA	High	Medium	Low	Medium
	h. Details of the reconstructed parts										
Photoscan	High	High	High	Medium	Medium	Low	Medium	High	Medium	High	High
OMR	High	High	High	High	Low	Medium	High	High	High	High	High
MVE	High	High	Medium	Medium	NA	NA	NA	High	Medium	Low	High
	i. Recognizability of the scene										
Photoscan	High	High	High	High	High	Low	High	High	Medium	High	High
OMR	High	High	High	High	Medium	Medium	High	High	High	High	High
MVE	High	High	High	High	NA	NA	NA	High	High	Low	High
	l. Realism										
Photoscan	High	High	High	Medium	Medium	Low	Low	High	Medium	High	High
OMR	High	High	High	High	Low	Low	High	High	High	High	High
MVE	High	High	Medium	Medium	NA	NA	NA	High	Low	Medium	High

Table II. Performance comparison between Open Mesh Reconstruction - using alternatively NVIDIA Titan XP GPU (OMR) and 16 virtual CPUs (OMR-CPU) -, Agisoft Photoscan on GPU, and the Multi-View Environment+MVS-Texturing pipeline (MVE) on GPU, across our test cases. Qualitative reconstruction assessment in sub-tables f-l is the most assigned label by three human evaluators.

DOI: 10.1002/cpe